Acido-Base Behavior of Hydroxamic Acids: Experimental and Ab Initio Studies on Hydroxyureas

Ivana Vinković Vrček, Ivan Kos, Tin Weitner, and Mladen Biruš*

University of Zagreb, Faculty of Pharmacy and Biochemistry, Kovačića 1, 10000 Zagreb, Croatia

Received: June 4, 2008; Revised Manuscript Received: September 22, 2008

The values of K_a, ΔS_a, and ΔH_a for deprotonation of hydroxyurea (HU) and *N*-methylhydroxyurea (NMHU), as targeted compounds, and for betainohydroxamic acid, were potentiometrically determined. Although NMHU has two and HU even three deprotonation sites, the measurements confirm that they behave as weak acids with a single $pK_a \approx 10$. Comparison with analogous thermodynamic parameters previously determined for series of monohydroxamic acids reveals deviations from a ΔS_a, vs ΔH_a plot for HU and NMHU, raising the question of the dissociation site of hydroxureas in water. In addition to the deprotonation of the hydroxyl oxygen, ab initio calculations performed at the MP2/6−311++G(d,p) level of theory for these two compounds indicate a notable participation of the nitrogen deprotonation site in HU. The calculations for the isolated, monohydrate, trihydrate, and decahydrate molecular and anionic forms of hydroxyureas support the importance of hydrogen bonding in the gas and aqueous phases. The hydroxylamino nitrogen in HU is the most acidic site in water, contributing ∼94% to the overall deprotonation process at 25 °C. On the contrary, the hydroxylamino oxygen is by far the most favored deprotonation site in NMHU, contributing almost 100% in aqueous medium. The predicted participations of two deprotonation sites in HU, calculated at the MP2/6−311++G(d,p) level of theory, combined with the calculated relative reaction enthalpy and entropy for the deprotonation, satisfactorily explain the observed deviation from linearity of ΔH_a vs ΔS_a, plot. There is no such a simple explanation for acid−base behavior of NMHU.

Introduction

Hydroxamic acids (Scheme 1) are weak organic acids, produced by various living organisms which utilize their Fe(III)-chelates (siderophores) for transfer of iron from environment into the cells. Over the years, there has been considerable growth of interest in the chemistry of hydroxamic acids, owing to their biological activities and chelating properties,[1−6] which make them applicable in medicine as analgetics, anti-inflamatories,[7] collagenase inhibitors,[8] anti-infectives,[9] antibiotics,[10] anticancer agents,[11,12] and so forth. Hydroxyurea (HU, $R_1 = NH_2$, $R_2 = H$) is a hydroxamic acid that is increasingly used in human medicine. Despite its simple molecular structure, HU displays many biological activities and its pharmacology has drawn considerable attention. HU is a highly specific low-molecular inhibitor of ribonucleotide reductase, hence of DNA synthesis,[13] with a broad spectrum of antitumor effects.[14−16] Among others, HU significantly improves clinical outcomes in patients with sickle cell disease, and nowadays, it represents a new prospective treatment for this disease.[17,18]

A large number of papers dealing with theoretical and experimental aspects of hydroxamic acids' acidity have been published.[19−34] The complete investigation of the process requires comparison of the results obtained from both experimental measurements and theoretical calculations adapted for reproducing the experimental conditions. Low molecular weight hydroxamic acids have been used as a role model for investigation of larger, naturally produced hydroxamic acids. It has been speculated that the observed biological activities of hydroxamic acids might be related to the similarity between the NC═O structural segment and those in proteins.[35] Since hydroxamic acids contain the smallest unit C═ONH that can bind to the DNA helix,[19,20] knowledge of the favored ionization sites is important for understanding the role played by hydroxamic acids in biological processes and in cancer drug design, as well as in metal ion complexation.

There has been a considerable debate as to whether these compounds are nitrogen or oxygen acids.[21] It was reported that the electronic properties of the functional groups, R_1 and R_2, play a significant role in the ionization of hydroxamic acids.[22] In the course of our investigation of hydroxamic acid properties, here we report the potentiometric determination and theoretical calculations of K_a, ΔS_a, and ΔH_a for hydroxyurea and *N*-methylhydroxyurea (NMHU, $R_1 = NH_2$, $R_2 = CH_3$) as targeted compounds. Several reports of the single-temperature pK_a values for HU[36] and NMHU[37,38] are available in the literature, but the complete sets of thermodynamic parameters for ionization in aqueous solution have not been reported so far.

The ionization reactions we study can be delineated by a general equation (1).

$$R_1C(O)N(OH)R_{2(aq)} \rightleftarrows R_1C(O)N(O)R^-_{2(aq)} + H^+_{(aq)}; K_a = \frac{[H^+_{(aq)}] \times [R_1C(O)N(O)R^-_{2(aq)}]}{[R_1C(O)N(OH)R_{2(aq)}]} \quad (1)$$

For the sake of better consistency between our results and the literature regarding the ionization of the low-molecular weight hydroxamic acids, here we also report thermodynamic parameters for acetohydroxamic acid (AcHA, $R_1 = CH_3$, $R_2 = H$) and benzohydroxamic acid (BHA, $R_1 = C_6H_5$, $R_2 = H$) redetermined under our experimental conditions. Namely, the reported thermodynamic data for these two hydroxamic acids

* To whom correspondence should be addressed. E-mail: birus@pharma.hr.

10.1021/jp804925b CCC: $40.75
Published on Web 10/25/2008

SCHEME 1: Hydroxamic Acid

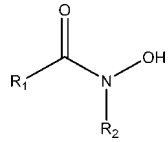

have been acquired in a different salt medium.[22] In an attempt to rationalize rather unexpected values of the obtained thermodynamic parameters for HU and NMHU (vide infra), we also report the potentiometric measurements on ionization of betainohydroxamic acid (BetHA, $R_1 = {}^{+}N(CH_3)_4$, $R_2 = H$), for which only a single-temperature pK_a value has been reported in literature.[39]

Finally, to facilitate interpretation of our experimental results, we have undertaken quantum chemical calculations of electronic structures and energies for HU and NMHU. Previously, HU and some of its *N*-substituted derivatives were studied theoretically,[26−29] but this is the first detailed theoretical study of NMHU. The already reported acidities were calculated without referring to the above thermodynamic state functions; whereas in this paper, we also present a detailed theoretical−thermodynamic study of deprotonation processes of hydroxyureas in the gas phase. An attempt to predict deprotonation processes in aqueous phase is also presented as a possible prototype for more complex systems, having in mind that if methods for predicting pK_a's can be calibrated on known systems, then it should be possible to predict acidities of more complex systems. Since we recently reported quantum-chemical description of complexation of vanadium(V) with hydroxyurea,[40] a detailed theoretical description of deprotonation reactions reported in this paper could also be taken as a step further toward the modeling of complexation reactions which are important in the environment.

Computational Methodology. The *Gaussian03* program package[41] has been employed in all of the calculations. Solvent effects in water have been calculated by means of the Tomasi's polarized continuum model (PCM)[42] in which the solvent is considered as a continuum dielectric, characterized by a constant permittivity. This method has been implemented in a number of forms with, for example, different choices for the definition of the solute−solvent dielectric boundary.[43] The method has been shown to be surprisingly accurate at calculating solvation energies, solvent-phase geometries, and other properties that do not depend strongly on explicit molecular solvent effects. Due to the controversial capability of PCM method for describing the effect of formation of hydrogen bonds between the solvent and solute, the intermolecular solvent−solute interactions were taken into account by explicit incorporation of water molecules. Thus, the solvent effects are considered in two ways. Since, in ab initio study of the formohydroxamic acid[31] and small aminoacids,[32] the clusters of up to three water molecules were investigated, we also performed calculations for clusters with one and three water molecules. In addition, we extended our investigation to the solute species microsolvated with ten water molecules. The energies and structures of AH•H_2O, AH•$3H_2O$, AH•$10H_2O$, A^-•H_2O, A^-•$3H_2O$, and A^-•$10H_2O$ were initially determined in the gas phase and afterward the PCM calculations were performed for each microsolvated species.

Owing to high computational costs, the calculations on clusters with ten water molecules presented in this work were carried out employing 6−311G(d,p) basis set with no added diffuse functions at the MP2 level of theory. Using quantum chemistry for manual exploration of each of the many hundreds of possibilities for these clusters is an uninviting task, uncertain in its outcome. The rigorous manual solution of the lowest-energy isomer of the decahydrated clusters surely would be precluded by the enormous labor required. There have been many efforts to deal with problems of similar complexity using automated procedures, but generally with the objective of finding the global minimum.[44] Fortunately, Saunders's fast, comprehensive, and automated "kick" method[45] (the method analogous to the stochastic random search procedure for finding conformers previously developed and extensively used for molecular mechanics surfaces)[46] through stochastic methodology produces isomers and conformers simply and effectively with little thought or effort, and its intensive application virtually ascertain finding of all the structures of the decahydrates.

To convert calculated H-bonding energies properly into enthalpies and free energies, corrections had to be done for the basis set superposition error (BSSE).[47] One most usually corrects for BSSE using counterpoise (CP) correction.[48] Vibrational frequencies were calculated on the CP-optimized PES[49] using the harmonic approximation as programmed in *Gaussian03* at the MP2/6−311++G(d,p) level of theory. The natural bond orbital (NBO) analysis has been carried out for the optimized structures at the MP2/6−311G(d,p) and MP2/6−311++G(d,p) levels of theory using the same basis set by NBO 3.1 program[50] as implemented in the *GAUSSIAN03* package.

Results and Discussion

Potentiometric Measurements. The values of acid dissociation constants (K_a, represented by eq 1) determined for HU, NMHU, BetHA, AcHA, and BHA at various temperatures in aqueous solution of constant ionic strength (2 M $NaClO_4$) are listed in Table 1.

The van't Hoff plots for ionization of hydroxamic acids and the calculated respective values of ΔH_a and ΔS_a are shown in Figure 1 and Table 2, respectively, whereas comparison of our results with the Crumbliss' data is shown in Figure 2.

Figure 2 clearly illustrates that our results for deprotonation of AcHA and BHA deviate acceptably from the theoretical line defined by Crumbliss and co-workers, indicating consistency between the results reported from the two laboratories regardless of the salt medium utilized (sodium perchlorate and nitrate, respectively).[22,51−53] On the contrary, the thermodynamic parameters determined for ionization of HU, NMHU, and BetHA exhibit a significant deviation from the straight line, thereby HU and NMHU exhibiting upward and BetHA downward deviations that exceed the experimental error limits.

Crumbliss and co-workers attributed the observed variations in ΔH_a and ΔS_a to the interactions of water solvent with the −[C(=O)NO^-]− hydroxamate moiety, i.e., to the differences in solvation of the anions. For BetHA, the obtained deviation from the experimentally defined straight line could be plausibly explained by taking into account the charges of studied hydroxamic acids. While all other hydroxamic acids in series are molecules, BetHA is a cation $(CH_3)_3N^+CH_2CONHOH$ which upon the deprotonation, unlike the other hydroxamic acids which form the anions, forms a zwitterion $(CH_3)_3N^+$-CH_2CONHO^-. Therefore, upon the deprotonation of BetHA, a strongly solvated cation is replaced by an overall neutral zwitterion which, although dipole−dipole stabilized in water, is expected to be solvated to a lesser extent than the anions formed upon deprotonation of other hydroxamic acids in the series. Thus, the observed deviation from the linearity for BetHA could be anticipated mainly based on the reaction entropy.

The anticipated deflection of the ionization reaction entropy, combined with the confirmed reliability of our experimental

TABLE 1: Temperature Dependencies of Ionization Constants, K_a,[a] of Investigated Hydroxamic Acids at $I = 2$ M ($NaClO_4$)

compd	log K_a (20 °C)	log K_a (25 °C)	log K_a (30 °C)	log K_a (37 °C)	log K_a (45 °C)
HU	−10.17 ± 0.09	−10.15 ± 0.09	−10.13 ± 0.09	−10.11 ± 0.09	−10.06 ± 0.09
NMHU	−9.81 ± 0.08	−9.79 ± 0.07	−9.78 ± 0.06	−9.76 ± 0.06	−9.74 ± 0.07
BetHA	−6.81 ± 0.01	−6.76 ± 0.02	−6.72 ± 0.02	−6.67 ± 0.02	−6.62 ± 0.02
AcHA	−8.90 ± 0.02	−8.86 ± 0.01	−8.82 ± 0.01	−8.80 ± 0.01	−8.78 ± 0.01
BHA	−8.34 ± 0.01	−8.31 ± 0.02	−8.27 ± 0.02	−8.22 ± 0.02	−8.19 ± 0.01

[a] Hereafter, the uncertainties have meaning of the single standard deviations, σ, of the reported parameter.

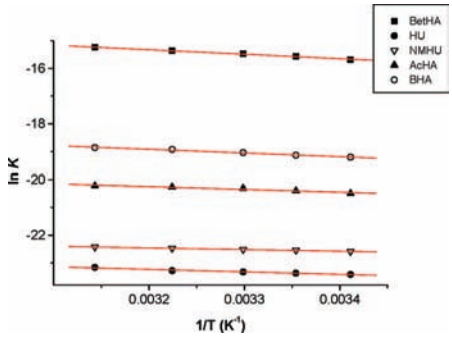

Figure 1. Van't Hoff plots for investigated hydroxamic acids at $I = 2$ M ($NaClO_4$).

TABLE 2: ΔH_a and ΔS_a for Deprotonation of Investigated Hydroxamic Acids at $I = 2$ M ($NaClO_4$)

hydroxamic acid	ΔH_a (kJ mol^{-1})	ΔS_a (J K^{-1} mol^{-1})	r	ΔH_a(est.) (kJ mol^{-1})[a]	ΔS_a(est.) (J K^{-1} mol^{-1})[a]
HU	7.55 ± 0.70	−169.0 ± 2.3	0.987	0	−141
NMHU	4.88 ± 0.21	−171.1 ± 0.7	0.997	−1	−150
BetHA	13.43 ± 0.52	−84.4 ± 1.7	0.998	23	−120
AcHA	8.43 ± 1.31	−141.4 ± 4.2	0.966	7	−138
BHA	11.14 ± 0.71	−121.6 ± 2.3	0.994	13	−128

[a] Calculated from the theoretical line in Figure 2, defined by Crumbliss and co-workers: $\Delta H_a = (0.28 \pm 0.01)$ kK × ΔS_aJ K^{-1}mol^{-1} + (47 ± 1) kJ mol^{-1}. ΔH_a(est.) and ΔS_a(est.) calculated assuming no deviation from the linearity of the experimentally obtained ΔS_a, or ΔH_a, respectively. The estimated uncertainties corresponding to the 95% confidence limit for the estimated ΔH_a and ΔS_a values are ~5 kJ mol^{-1} and ~17 J K^{-1} mol^{-1}, respectively.

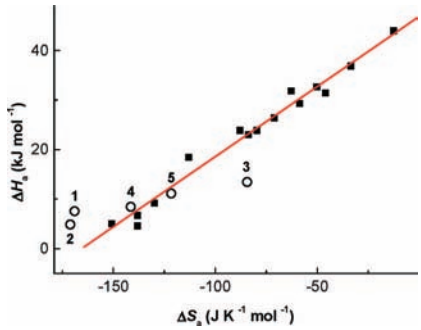

Figure 2. Plot of ΔH_a vs ΔS_a for investigated hydroxamic acids at $I = 2$ M. Full squares are data from refs 22, 51, 52 and 53. Open circles: **1**(HU), **2**(NMHU), **3**(BetHA), **4**(AcHA), and **5**(BHA).

results, indicates that the deviation from the theoretical straight line obtained for BetHA should not be considered as an experimental error. Consequently, this also advocates the obtained deviations for HU and NMHU not to be qualified as experimental errors. Instead, a plausible explanation must be looked for that would clarify whether the deviations are related to the reaction entropies or enthalpies.

Although the observed deviations of reaction entropy for ionization of HU and NMHU could be rationalized in several ways, all plausible rationales must comprehend either relatively small molar entropies of HU and NMHU in comparison with other hydroxamic acids in the series, or a relative small decrease of entropy upon their ionizations in solution.

As discussed previously,[53] differences in the hydration Gibbs free energies among the undissociated acids are expected to be of minor importance while the hydration of anions is expected to be of crucial importance. The delocalization of the N1 atom lone pair of electrons is expected to play a fundamental role in causing variations in solvent ordering about the hydroxamate anion mainly caused by an increase of net dipole moment. It seems worth noting that, owing to the electron delocalization between C and N2 atoms, hydroxyureas have one more probable resonant form than that of the rest of hydroxamic acids in series. This in turn raises the importance of the solvent interactions not only with the hydroxamate moiety but also with other functionalities in molecules and ions of hydroxamic acids. Furthermore, since the structural and theoretical studies have demonstrated the relevance of the hydrogen bonding effects in monohydroxamic acids,[24] one possible explanation could be based on the differences in the intra- and/or intermolecular hydrogen bonding. Absence of a hydrogen-bonded dimer in solution, confirmed by determination of ionization constants at two different analytical concentrations of the compounds (a 10-fold decrease of the hydroxamic acids concentration affords calculation of essentially unchanged pK_a values), leaves only the solute−solvent hydrogen bonding to be considered.

Alternatively, relating the observed deviations to the reaction enthalpies mainly imposes the change in deprotonation sites, or in other words, recognition of the nitrogen as well as the oxygen as a deprotonation site of hydroxyureas.

Quantum Chemical Calculations. In attempt to resolve the above ambiguity, we have carried out a computational study on HU and its *N*-methyl derivative. For each compound, three different aspects are investigated with appropriate computational methods. The first aspect concerns the relative stabilities of the neutral and anionic forms of the investigated molecules in the gas phase and solution. The second aspect concerns structural and electronic properties of the neutral and anionic forms of compounds as well as the nature of the specific intra and intermolecular hydrogen-bonding interactions. The third aspect concerns the deprotonation processes of isolated molecules and water adducts in solution. Calculations for aqueous medium were performed by using PCM model, but regarding the weakness of PCM method to reproduce specific interactions with the surrounding solvent molecules such as long-lived hydrogen bonds, the solvent effects were modeled by an explicit account of the solvent molecules in addition to the continuum medium model. Gas-phase ab initio SCF studies on a microsolvate of HU with one water molecule revealed ionizable protons of HU molecule to be involved in the hydrogen bonding.[33] We have extended the theoretical calculations by incorporating two and nine more water molecules into the solvation shell of molecular and anionic forms of HU in gas-phase and in the polarized

SCHEME 2: Conformers of HU

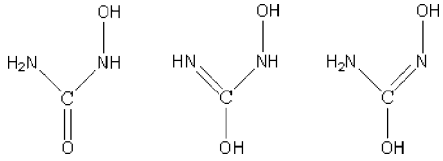

continuum to explore how these incorporations modify relative stabilities, geometries, and ionization properties of HU through the hydrogen bonding.

Hydroxyurea. HU has been extensively studied at the various computational levels.[25,28−30] It is known that HU exists as keto and iminolic isomers (Scheme 2), the keto conformer being far more stable form in the gas phase and in aqueous solution. The greater stability of the amide form is mainly caused by electronic factors related to the exceptional stability of the carbonyl group.[54]

As the experimental evidence[23,55] and previous theoretical calculations[56] of the molecular structure of hydroxamate moieties reveal that these functional groups exist in the more stable keto form, all calculations in this work were carried out only on this tautomer. The results of our calculations are shown in Tables S1−S5 of the Supporting Information. Since HU may undergo deprotonation at the hydroxylamino oxygen (U^-O1) and nitrogen atoms (U^-N1) as well as at the amino nitrogen (U^-N2), the calculations were performed for all of the deprotonation sites. However, the potentiometric experiments reveal only one pK_a value, therefore no calculation was carried for double deprotonated species.

We have calculated the geometries and energetics of various molecular and anionic forms of HU at the MP2/6−311++G(d,p) level of theory, which by dealing with the diffuse MO, should be more suitable especially for calculations of organic anions. Furthermore, in order to improve estimation of the intermolecular interaction energies of the molecular and even more so of the anionic forms of HU-water clusters, the energetics of cluster species was further refined at the BSSE[48] corrected second-order Møller−Plesset perturbation theory (MP2) level. The CP correction removes an artificial attractive force between the fragments, and the O···H distances increase upon CP optimization. The changes in these distances can be quite large (up to 0.28 Å). Even with the large 6−311++G(d,p) basis set applied, the BSSE is still substantial. The counterpoise-corrected relative Gibbs free energies modify relative stability of species under study (as can be seen from Tables 3 and 4). The correction introduces larger differences in relative Gibbs free energy of anionic species in comparison to the CP-uncorrected results (Table S1 of the Supporting Information). However, for reasons mentioned above, the MP2/6−311++G(d,p) level of theory was not applied to the decahydrates, and hence, comparison of those to other microsolvated species is impossible at that level.

The fact that proton transfer between −COOH and $-NH_2$ groups, to produce $-COO^-$ and $-NH_3^+$, occurs in crystal structures and in aqueous solution of amino acids guided us to examine the conformational and energetic properties of zwitterionic forms of HU as well. The calculated molecular geometries of the zwitterionic forms of isolated, monohydrated, and trihydrated HU were compared to the corresponding molecular forms of HU. It is interesting to note that at the MP2/6−311++G(d,p) level, most of the starting structures of hydrated zwitterionic species of *E*-HU converged to the nonzwitterionic forms by the spontaneous intramolecular proton transfers (Figures 3 and 5). Unlike for amino acids, large calculated energy gaps between most of the nonzwitterionic and zwitterionic forms indicate a strong preference for nonzwitterionic HU (see Tables 3 and S1 of the Supporting Information), which can be accounted for by a stronger basicity of $-N(H)O^-$ than COO^- moiety.

The results at the MP2/6−311++G(d,p) level of theory corrected for BSSE, shown in Table 3, reveal for the isolated and monohydrate species in gas phase that *E*-molecular forms of HU dominates over the *Z*-forms by more than 11 kJ mol^{-1}. Although the isolated *Z*-HU molecule appears more suitable for the intramolecular hydrogen bonding than *E*-HU, lower free energy of the latter is possibly indicative of both, importance of the charge separation located on two oxygen atoms in molecule and of importance of the dipole moment decrease (Tables S3 and S5 of the Supporting Information). Only in the trihydrate species, dipole moments of both forms become closer to each other and the free energies of the *E*- and *Z*-form of trihydrates almost equal. The CP corrections decrease the intermolecular hydrogen bonding with water molecules in *Z*-form, making eventually this form 4.7 kJ mol^{-1} less stable than *E*-form. Immersion into the continuum changes only the stability order of the trihydrate clusters, among which *Z*-HU becomes slightly more stable than *E*-HU trihaydrate.

In the case of the isolated and the microsolvated anions, *Z*-U^-N1 forms are the most stable in the gas phase and CP corrections cause no change in stability orders (Table 4). After the immersion in the continuum, the stability order remains the same for the isolated and monohydrate species. In the case of trihydrate clusters, the stability order changes and *E*-$U^-O\cdot 3w$ becomes the most stable species among the microsolvated anions. As expected, the CP corrections significantly decrease the intermolecular hydrogen bonding within the trihydrates.

In order to obtain some information regarding the influence of an extended number of associated water molecules on the stability order among the species, the geometries and energetics of various molecular and anionic forms of HU at the MP2/6−311G(d,p) level of theory were also calculated (Table S6 of the Supporting Information). Namely, at an applied level of theory, it was possible to perform calculations for up to 10 water molecules. It is interesting to note that inclusion of 10 water molecules in the clusters significantly decreases the energy difference between the *E*- and *Z*-forms of HU but still in favor of *E*-HU·10w. The small difference in energy of molecular decahydrates is possibly due to a large energy-decrease contributed by the water−water intermolecular hydrogen bonding, which entirely outbalance the hydrogen bonding between HU and water molecule(s) making its contribution to the overall energy less important. The same level of theory predicts the hydroxamate hydroxyl oxygen, *E*-$U^-O\cdot 10w$, as the most stable (4.7 kJ mol^{-1}) decahydrate deprotonation site. A sketch of some important neutral and anionic complexes of HU with ten water molecules is shown in Figure S1 of the Supporting Information.

All the above-mentioned results of calculations at the MP2/6−311++G(d,p) level of theory were intended to obtain suitable thermodynamic parameters for characterization of deprotonation of HU and NMHU. However, in order to make reliable comparison, all of the calculated values of free energy must be expressed in a mutually comparable way. For each particular molecular or anionic species, the Gibbs free energy, G_{tot}, is therefore expressed according to eq 2.

$$G_{tot} = G_{species} + NG_{water} \quad (2)$$

where for the isolated, monohydrate, and trihydrate species *N* equals 3, 2, and 0, respectively. Furthermore, in order to take

TABLE 3: Calculated Gibbs free energies, G_{tot}, and relative Gibbs Free Energies, ΔG,[a] for Various Molecular Forms of HU at 298.15 K Calculated in the Gas Phase and Water Solution at the MP2/6-311++G(d,p)[b]

	gas-phase		PCM		gas-phase (CP-corr.)		PCM (CP-corr.)	
	G_{tot}	ΔG	G_{tot}	ΔG	G_{tot}	ΔG	G_{tot}	ΔG
E-HU	−528.540128	0.0	−528.562924	11.4	−528.536496	2.6	−528.564313	2.1
Z-HU	−528.534534	14.7	−528.559125	21.3	−528.530902	17.3	−528.560514	12.0
Z-HU_{zw}	−528.444728	250.2	−528.496001	186.9	−528.441096	252.8	−528.497390	177.6
E-HU·w	−528.539798	0.9	−528.567252	0.0	−528.537491	0.0	−528.565097	0.0
E-HU_{zw}·w	−528.535575	11.9	−528.561080	16.2	−528.532200	13.9	−528.561080	10.5
Z-HU·w	−528.535168	13.0	−528.561751	14.4	−528.531244	16.4	−528.560125	13.0
Z-HU_{zw}·w	−528.450202	235.9	−528.501683	172.0	−528.445787	240.5	−528.500868	168.5
E-HU·3w	−528.539447	1.8	−528.557448	25.7	−528.531727	15.1	−528.556174	23.4
E-HU_{zw}·3w	−528.490414	130.4						
Z-HU·3w	−528.540006	0.3	−528.554018	34.7	−528.529919	19.9	−528.553702	29.9
Z-HU_{zw}·3w	−528.474661	171.7						

[a] Difference between the formation Gibbs free energy of various molecular forms of HU and the most stable molecular form of HU, respectively. [b] Gibbs free energies are given in a.u., relative Gibbs free energies are given in kJ mol^{-1}. For the isolated, monohydrate, and trihydrate species *N* equals 3, 2, and 0, respectively.

TABLE 4: Calculated Standard Gibbs Free Energies, G_{tot}, and Relative Gibbs Free Energies, ΔG,[a] for Various Anionic Forms of HU at 298.15 K Calculated in the Gas Phase and Water Solution at the MP2/6-311++G(d,p) Theory Level[b]

	gas-phase		PCM		gas-phase (CP-corr.)		PCM (CP-corr.)	
	G_{tot}	ΔG	G_{tot}	ΔG	G_{tot}	ΔG	G_{tot}	ΔG
E-U^-N1	−527.972193	103.5	−528.079528	33.0	−527.968561	83.3	−528.080917	27.1
E-U^-O	−527.972934	101.5	−528.077159	39.2	−527.969302	81.4	−528.078548	33.3
E-U^-N2	−527.982078	77.6	−528.079049	34.2	−527.978446	57.4	−528.080438	28.3
Z-U^-N1	−527.983476	73.9	−528.084710	19.4	−527.979844	53.7	−528.086099	13.5
Z-U^-O	−527.953579	152.3	−528.068717	61.3	−527.949947	132.1	−528.070106	55.4
Z-U^-N2	−527.980188	82.5	−528.076613	40.6	−527.976556	62.3	−528.078002	34.7
E-U^-N1·w	−527.985915	67.5	−528.088204	10.2	−	−	−	−
E-U^-O·w	−527.991069	54.0	−528.089071	8.0	−527.987126	34.6	−528.088337	7.6
E-U^-N2·w	−527.989376	58.4	−528.081585	27.6	−527.974925	66.6	−528.080799	27.4
Z-U^-N1·w	−527.995988	41.1	−528.092104	0.0	−527.993378	18.2	−528.091233	0.0
Z-U^-O·w	−527.973998	98.8	−528.080832	29.6	−527.968557	83.3	−528.078014	34.7
Z-U^-N2·w	−527.992205	51.0	−528.084417	20.2	−527.988847	30.1	−528.083727	19.7
E-U^-N1·3w N1·3w	−528.005974	14.9	−528.082067	26.3	−527.990666	25.3	−528.078038	34.6
E-U^-O·3w	−528.009536	5.5	−528.086471	14.8	−527.997165	8.3	−528.087365	10.1
Z-U^-N1·3w N1·3w	−528.011648	0.0	−528.086083	15.8	−528.00032	0.0	−528.082438	23.1
Z-U^-O·3w	−528.003814	20.5	−528.086589	14.5	−527.987784	32.9	−528.081973	16.7

[a] Difference between the formation Gibbs free energy of various anionic forms of HU and the most stable anionic form of HU, respectively. [b] Gibbs free energies, calculated according to eq 2, are given in a.u. Relative Gibbs free energies are given in kJ mol^{-1}.

into account the stabilization attained by the hydrogen bonding among the water molecules, the calculations were performed for a single water molecule, as well as for the binary and ternary water clusters. The free energy for H_2O calculated at MP2/6−311++G(d,p) level of theory in aqueous phase is −76.265559 au, while the CP-corrected values at the same level of theory for $(H_2O)_2$ and $(H_2O)_3$ are, −152.550193 au and −228.819280 au, respectively. These values correspond to the formation Gibbs free energies of −50.0 kJ mol^{-1} and the of −59.3 kJ mol^{-1} for $(H_2O)_2$ and $(H_2O)_3$, respectively.

The values calculated according to eq 2 are shown in Tables 3 and 4. The results reveal how calculated free energies of various species depend on whether (i) the PCM model was directly applied on the particular trihydrate adduct, or (ii) the model was applied on the particular isolated species or the monohydrate adduct in combination with Gibbs free energy for the ternary and binary water clusters, respectively.

At the CP-corrected MP2/6−311++G(d,p) level of theory, eq 2 predicts *E*-monohydrate adducts and *E*-isolated species as the most stable molecular forms in water. The lowest energy monohydrate molecule, *E*-HU·w, is only 2.1 kJ mol^{-1} separated from isolated molecule, *E*-HU, indicating only a bit stronger hydrogen bonding between HU and H_2O than the average hydrogen bonding within the three-water cluster. A further addition of water molecules destabilizes the *E*-dihydrate indicating that three water molecules are more favorably H-bonded between themselves. Interestingly, while the *E*-monohydrated

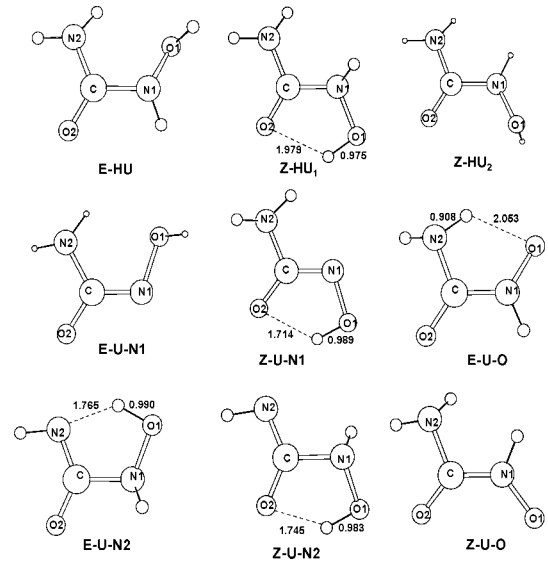

Figure 3. The most stable molecular and anionic gas-phase forms of isolated hydroxyurea optimized at the MP2/6−311++G(d,p) level of theory. The distances are given in Å.

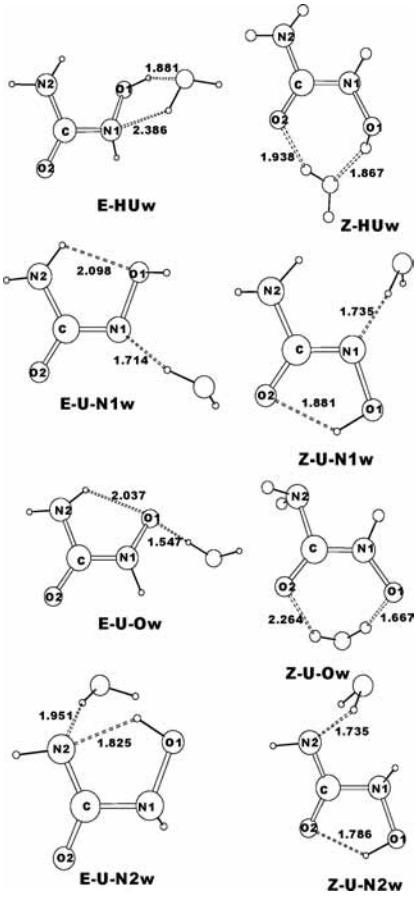

Figure 4. Complexes of neutral and anionic forms of HU with one water molecule optimized at MP2/6−311++G(d,p) level of theory. The distances are given in Å.

zwitterion exhibits the stability, *Z*-zwitterions are very unstable possibly due to the easily feasible proton-transfer between the $-NH_2$ and $-NOH$ groups, which are in the latter geometry oriented closer to each other. Yet, in the calculated speciation of HU, contribution of even the most stable zwitterion is no more than 1%. Although the *z* form of HU molecule exhibits much larger dipole moment than the *e* form, the calculated difference of 12 kJ mol^{-1} in Gibbs free energies corresponds to a molar ratio of >100 in favor of the *E*-HU forms. According to NBO analysis, intramolecular hydrogen bonding between the hydroxyl oxygen and amine hydrogen in *E*-form is ∼3 kJ mol^{-1} stronger than the intramolecular hydrogen bonding between the carbonyl oxygen and hydroxyl hydrogen in *Z*-form. Addition of a single water molecule precludes intramolecular hydrogen bonding in *Z*-monohydrate. The rest of *E*-HU stabilization comes largely from the exceptional delocalization of the free electron pairs of nitrogen and carbonyl oxygen atoms into the C−N and C−O antibonding orbitals. It is interesting that calculation yields no electron density delocalization neither from the carbonyl nor hydroxyl O atoms to N−H NBO* orbitals, indicating only electrostatic attractions between these atoms (Wiberg NAO bond index = 0.001). NBO analysis show that the water molecules in *E*-HU·w and *Z*-HU·w are hydrogen bonded through the hydroxyl −NO*H* and the water O atoms, decreasing the energy by ∼25 kJ mol^{-1} and 31 kJ mol^{-1}, respectively. As expected from the above discussion, each of these two energies is smaller than the H-bonding energy in $(H_2O)_2$, confirming the predictive capability of NBO analysis. However, a slightly stronger hydrogen bonding in *Z*-form than in *E*-form does not compensate weaker stabilization achieved by the electron delocalization. Total non-Lewis structures, as indicators of delocalizing interactions determined by a second-order perturbation approach, for *e* and *z* molecules are 1.31% and 1.28%, respectively, indicating a higher total resonance delocalization in *E*-HU than in *Z*-HU. For the total of 40 electrons, this corresponds to a difference in the natural population changes of 0.012 e$^-$, while the change of ∼0.001 e$^-$ corresponds to the energy change of ∼2.5 kJ mol^{-1}.[57] The level of resonance delocalization in trihydrate clusters has been increased up to 1.426% and 1.361% for the *E*- and *Z*-trihydrates, respectively, and the calculated total stabilizations through H-bonding with 3 water molecules are for both the *E*- and *Z*-trihydrate, ∼26 kJ mol^{-1}. Nevertheless, all of this energy decrease in the trihydrates cannot compensate for the decrease achieved by the hydrogen bonding between the three water molecules.

Table 4 lists analogous results for the anionic species of HU. The stability order defined at the MP2/6−311++G(d,p) level of theory indicates that the preferable deprotonation site in HU is the hydroxylamine nitrogen. The most stable anion, *Z*-U$^-$N1·w, is 7.6 kJ mol^{-1} more stable than that deprotonated at the hydroxylamino oxygen atom, *E*-U$^-$O·w. Both ions are ∼27 kJ mol^{-1} more favorably hydrogen bonded with the water molecule than two water molecules to each other. Interestingly, further addition of water molecules destabilizes the clusters, indicating that only one water molecule satisfies the anions' H-bonding capacity. The *E*-U$^-$N1 anion is resonantly stabilized by the delocalization of the free electron pairs from carbonyl oxygen and amino nitrogen atoms into the empty σ^*_{C-N1} molecular orbital, and from delocalization of the free electron-pairs from carbonyl oxygen and N1 into the σ^*_{C-N2} molecular orbital. However, the main resonance stabilization of *E*-U$^-$O1 anion comes from the delocalization of the nitrogen atoms free electron-pairs into the carbonyl $\sigma_{C=O2}$ molecular orbital, while the delocalization of the oxygen free electron pairs atoms into the σ^*_{C-N1} and σ^*_{C-N2} molecular orbitals contributes significantly less. Like in molecules, inclusion of even one water molecule prevents the intramolecular H-bonding, but leaves the basic resonance stabilization of the mono- and trihydrate almost unchanged. Delocalization of a free electron pair from carbonyl oxygen into the water NBO-antibonding molecular orbital yields strong hydrogen bonding stabilization in the monohydrate, though the total H-bonding in the trihydrate is somewhat stronger than in the monohydrate. From the resultant energy difference between the most stable anionic forms of hydroxyurea in aqueous solution, a 16:1 molar ratio in favor of Z-U$^-$N1·w over (*E*-U$^-$O·w + *E*-U$^-$O·3w) can be calculated.

***N*-Methylhydroxyurea.** . There have been a few theoretical studies of *N*-alkyl derivatives of HU,[27,58] but to the best of our knowledge no such study was reported for NMHU. Unlike HU, NMHU has only two possible conformers shown in Scheme 3. The results reveal a ∼20 kJ mol^{-1} energy difference between the least stable keto conformer and the most stable iminolic conformer, calculated as isolated molecules at the DFT level with triple-ζ split valence basis set.[30] Therefore, in agreement with a general suggestion regarding hydroxamic acids based on the experimental evidence,[54] we can confidently argue that only the *Z*- and *E*-keto conformers of NMHU are essentially present in aqueous solution. In turn, there are only two deprotonation sites of NMHU; one at the hydroxylamino oxygen (U$^-$O1) and second at the amino nitrogen (U$^-$N2).

Since there is no available data in literature, we have fully optimized all possible structures of neutral and anionic forms of NMHU. Interestingly, every attempt to locate a complex between an anion deprotonated on N2 with three water

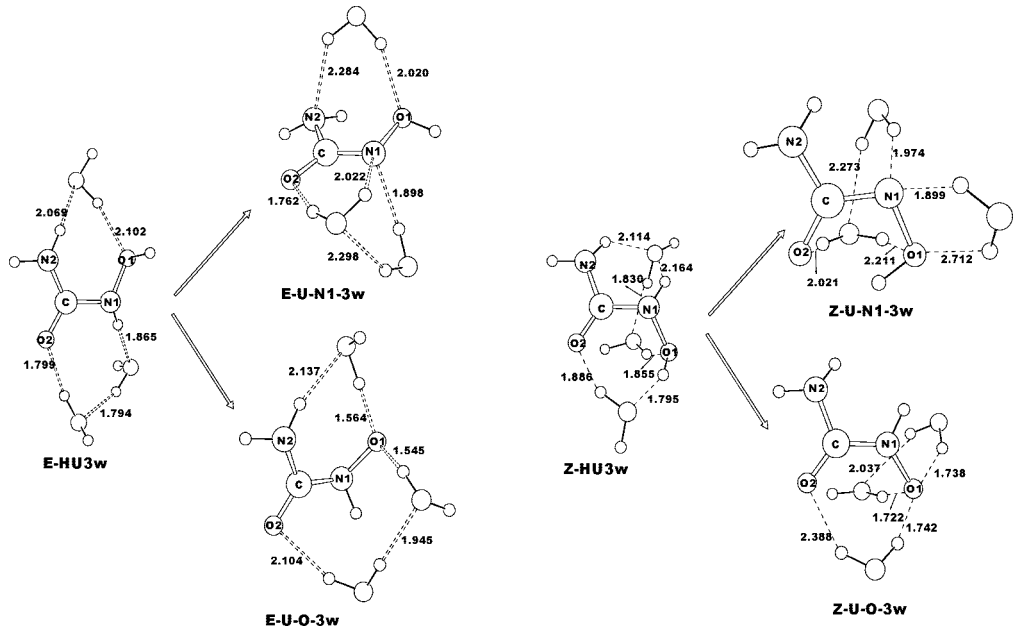

Figure 5. The most stable complexes of neutral and anionic forms of HU with three water molecules optimized at MP2/6−311++G(d,p) level of theory. The distances are given in Å.

SCHEME 3: Conformers of NMHU

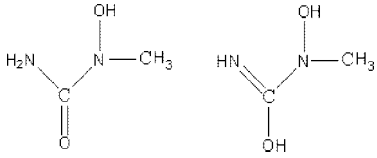

molecules failed, either due to convergence failures or due to rearrangement processes leading from an N2-deprotonated starting structure to an O1-deprotonated anion during optimization. The results of our calculations are shown in Tables 5, S7 and S8 of the Supporting Information. Figure 6 shows the most stable isolated and cluster species of molecular and anionic forms of NMHU optimized at the MP2/6−311++G(d,p) level of theory.

In the case of *e* molecular forms of NMHU, all zwitterionic starting structures converged to nonzwitterionic form (Figure S2 of the Supporting Information). Only the isolated *Z*-NMHU zwitterionic structure survived optimization procedure at the MP2/6−311++G(d,p) level of theory, but was destabilized more than those of HU, exceeding 200 kJ mol^{-1} increase compared to the Gibbs free energy of the corresponding nonzwitterionic structures. A plausible explanation one can offer is the bulkiness of the *N*-methyl substituent that prevents the proton transfer from −OH to $-NH_2$ group.

The results reveal again the *E*-form as the most stable. *E*-NMHU·w is the most stable among the molecular species, but with the free energy of *E*-NMHU being higher only 1.9 kJ mol^{-1}. Like for HU, the immersion of species from gas phase into the continuum causes neither additional dramatic change in geometries nor in the stability order among the molecular forms of NMHU. Among the anions, *E*-NMU$^-$O·3w appears to be by far the most stable, with the closest in energy among *Z*-anions, *Z*-NMU$^-$O·3w, being higher 26.1 kJ mol^{-1}.

The Gibbs free energies of isolated neutral and anionic forms of NMHU are compared with that of monohydrates and trihydrates by using eq 2, and calculating the total Gibbs free energies (Table 5). In the case of NMHU, the PCM method applied to the trihydrate gives rather higher Gibbs free energies than when applied to the analogous HU species. Apparently, the hydrophobicity of the *N*-methyl group repels the water molecules even stronger, favoring hydrogen bonding rather among them selves. The lowest energy molecular form, *E*-NMHU·w, is only 1.9 kJ mol^{-1} separated from *E*-NMHU, indicating only a bit stronger hydrogen bonding between NMHU and H_2O than among the water molecules. The *E*-forms are nicely separated from the *z* analogs by 15.7 kJ mol^{-1} of Gibbs free energy, corresponding to a molar ratio of $\sim 10^3$:1 in favor of the *e* form of NMHU. The higher energy difference between the *Z*- and *E*-monohydrates of NMHU is on the line with the above assumption, i.e., the loss of intramolecular hydrogen bonding cannot be fully compensated by the intermolecular H-bonding to water molecule. According to NBO analysis, the main stabilization of *E*-form comes mainly from the free electron pairs donation from both nitrogen atoms into C═O bond. A lack of such stabilization in the *Z*-form is only partially compensated by the double intermolecular hydrogen bonding through delocalization of the free electron pair from the carbonyl oxygen into the water natural antibonding molecular orbital (19 kJ mol^{-1}) and through the free electron pair donation of the water O-atom to N−O*H* (∼36 kJ mol^{-1}). NBO analysis predicts for *E*-NMHU·w a single H-bonding of ca. 25 kJ mol^{-1} coming up from the free electron pair donation of the water O-atom into N−O*H*. Total non-Lewis structures for *e* and *z* molecules are almost equal, 1.213% and 1.215%, respectively, indicating a slightly higher total resonance delocalization in the *z* form of NMHU. For 48 electrons, this corresponds to a difference in the natural population changes of <0.001 e^- and a negligible energy difference.

The most stable anionic species in solution are *E*-NMU$^-$O·3w and *E*-NMU$^-$O·w, which are more stable than the *z* analogs by more than 26 kJ mol^{-1}. As in the case of molecular forms, the stability of the anionic *E*-forms mainly comes from a strong electron delocalization of the free electron pairs of both nitrogen atoms into C═O bond, which is significantly weaker in the *z* analogs. Counterpoise correction significantly changes stability ordering of molecular and anionic forms of NMHU and intermolecular distances generally increase when these complexes are optimized on a CP-corrected surface.[59,60]

TABLE 5: Calculated Gibbs Free Energies, $G_{species}$, and Relative Gibbs Free Energies, $\Delta G_{species}$,[a] for Various Molecular and Anionic Forms of NMHU at 298.15 K Calculated at the MP2/6-311++G(d,p) Level of Theory[b]

species	gas-phase			PCM		
	$G_{species} + NG_{water}$	$\Delta G_{species}$	$\Delta G_{species}$ (CP-corr.)	$G_{species} + NG_{water}$	$\Delta G_{species}$	$\Delta G_{species}$ (CP-corr.)
			molecular forms			
E-NMHU	−567.704798	0.00	11.8	−567.701166	0.0	1.9
E-NMHU·w	−567.704609	75.10	0.0	−567.700588	1.5	0.0
E-NMHU·3w	−567.699053	172.75	36.1	−567.689470	30.7	34.0
Z-NMHU	−567.700336	12.05	27.2	−567.696704	11.7	17.3
Z-NMHU·w	−567,698498	89.62	20.1	−567.693622	19.8	15.7
Z-NMHU·3w	−567.702074	157.34	42.2	−567.687381	36.2	39.0
			anionic forms			
E-NMU⁻N	−567.147209	83.7	27.2	−567.143577	54.2	22.1
E-NMU⁻N·w	−567.140467	101.4	29.4	−567.135000	76.7	33.2
E-NMU⁻O	−567.140653	100.9	31.1	−567.137021	71.4	26.0
E-NMU⁻O·w	−567.159308	51.9	0.0	−567.153287	28.7	1.3
E-NMU⁻O·3w	−567.179112	0.0	1.5	−567.164239[c]	0.0	0.0
Z-NMU⁻N	−567.14544	88.3	34.1	−567.141808	58.8	29.0
Z-NMU⁻N·w	−567.147059	84.1	30.3	−567.148757[c]	40.6	26.1
Z-NMU⁻O	−567.116568	164.1	61.2	−567.112936	134.6	56.1
Z-NMU⁻O·w	−567.138144	107.5	29.5	−567.131530[c]	85.8	33.7
Z-NMU⁻O·3w	−567.164156	39.2	27.5	−567.146610[c]	46.2	29.5

[a] Difference between the formation Gibbs free energy of various anionic forms of HU and the most stable anionic form of HU, respectively. [b] Gibbs free energies are given in a.u., relative Gibbs free energies are given in kJ mol^{-1}. For the isolated, monohydrate, and trihydrate species *N* equals 3, 2, and 0, respectively. [c] Gibbs free energies obtained from the single-point frequency calculations on the CP-corrected surfaces on the MP2/6−311++G(d,p) optimized structures.

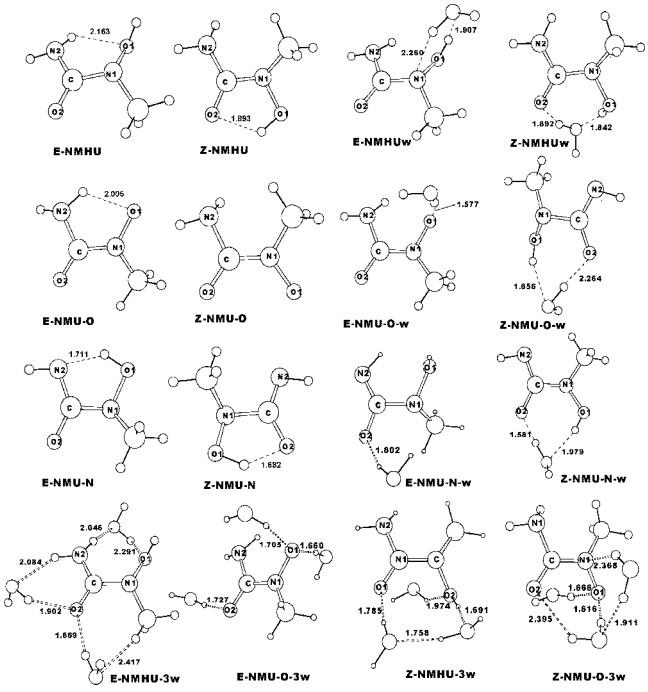

Figure 6. Most stable molecular and anionic gas-phase forms of the isolated, monohydrate- and trihydrate-*N*-methylhydroxyurea optimized at the MP2/6−311++G(d,p) level of theory. The distances are given in Å.

Calculation of Equilibrium Constants for Deprotonation Processes. HU may undergo deprotonation at the hydroxylamino oxygen (U⁻O1) and nitrogen atoms (U⁻N1) but also at the amino nitrogen (U⁻N2). The reported calculations carried out by Bagno and Comuzzi[26] predict the most stable ion in the gas phase to be U⁻N1, and our calculations at the MP2/6−311++G(d,p) level of theory confirm this prediction. The same authors have been investigated the ionization of various sites of HU in water solution, but experimental determination of the preferred deprotonation sites in these polyfunctional acids and bases is a formidable task, even though sometimes there is little doubt of the ionization site.[61] Initially, it was accepted that hydroxamic acids were *O*-acids,[22] but extensive IR and UV measurements in dioxane and aqueous alcohol solutions[62] indicate that hydroxamic acids are *N*-acids, a conclusion also supported by ^{17}O NMR and FT-IR studies of the benzohydroxamate ion in methanol.[63] Potentiometric measurements compatible with *O*- and *N*-deprotonation of hydroxamic acids have been also reported.[51,52,26,62,63] Dynamic NMR and NOESY (1D and 2D) experimental results obtained for different hydroxamic acids and their anions have shown that *N*- and *O*-deprotonations are possible.[64] The majority of the ab initio studies on acid−base properties of hydroxamic acids appear to confirm the N-acidity.[19,56,65] Most of these studies concern the smallest species, the formohydroxamic acid.[69,66]

SCHEME 4: Born−Haber Thermodynamic Cycle Used in the Calculation of pK_a

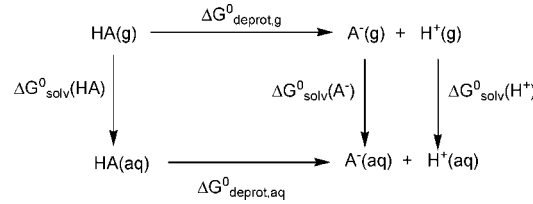

TABLE 6: Calculated Reaction Gibbs Free Energies for Selected Deprotonation Processes of HU and NMHU in the Gas Phase ($\Delta G^o_{deprot,g}$, in kJ mol^{-1}) and in Aqueous Solution ($\Delta G^o_{deprot,aq}$, in kJ mol^{-1}) with Corresponding pK_a Values in Water at 298.15 K at the MP2/6-311++G(d,p) Levels of Theory

process	$\Delta G^o_{deprot,g}$	$\Delta G^o_{deprot,aq}$	pK_a	pK_a (exp.)
E-HU ⇄ *Z*-U⁻N1 + H⁺	1433.8	123.7	21.7	10.2
E-HU·w ⇄ *Z*-U⁻N1·w + H⁺	1400.9	116.7	20.4	
E-HU·3w ⇄ *E*-U⁻O·3w + H⁺	1375.9	114.2	20.0	
E-NMHU ⇄ *E*-NMU⁻N + H⁺	1436.3	140.8	24.7	9.8
E-NMHU·w ⇄ *E*-NMU⁻O·w + H⁺	1409.3	123.5	21.6	
E-NMHU·3w ⇄ *E*-NMU⁻O·3w + H⁺	1351.4	107.1	18.8	

The theoretical prediction of deprotonation site and corresponding pK_a values continues to arouse a considerable amount of interest and there has been a large number of papers published in this area even over the last two years.[67] These papers have explored different systems, different solvents, and different aspects of the computational methods used to evaluate pK_a. Some of the papers have provided contrasting recommendations about the procedures to be used, but the recent work of Liptak and Shields[68−71] has established a well-defined protocol employing state-of-the-art molecular orbital theory, which has been shown to be highly accurate across a range of different chemical systems.

In order to calculate thermodynamic parameters for ionization reaction in water, thermodynamic parameters for hydration of each separate species must be combined with the gas-phase thermodynamic parameters for the deprotonation reaction. The standard Gibbs free energy of deprotonation of HA in water, $\Delta G^o_{deprot,aq}$, is defined according to the Born−Haber thermodynamic cycle presented in Scheme 4.

The standard Gibbs free energy of each species (HA, A^-, and H^+) in water (ΔG^o_{aq}; with respect to the reference state where all of the nuclei and electrons are completely separated from one another at 0 K in the gas phase) can be written as the sum of the gas phase standard Gibbs free energy, ΔG^o_g, and the standard Gibbs free energy of solvation in water, ΔG^o_{solv}, according to eqs 3 and 4:

$$\Delta G^o_{aq}(X) = \Delta G^o_g(X) + \Delta G^o_{solv}(X) \quad (3)$$

where X represents HA, A^-, or H^+ species.

The standard Gibbs free energy of each species, ΔG^o_g (X), in the gas phase at its standard state (ideal gas at 1 atm and 298.15 K)[72] is obtained by,

$$\Delta G^o_g = E_{0K} + \mathrm{ZPE} + \Delta\Delta G_{0\rightarrow 298K} \quad (4)$$

The total energy of the molecule at 0 K, E_{0K}, is calculated at the optimum geometry. The zero-point energy, ZPE, and the Gibbs free energy change from 0 to 298.15 K at 1 atm, $\Delta\Delta G_{0\rightarrow 298K}$, are calculated from the vibrational frequencies. Translational and rotational free energy contributions are also calculated in the ideal gas approximation.

The standard Gibbs free energy of H^+, ΔG^o_g (H^+), has been taken from the literature as $\Delta G^o_g(H^+) = 2.5RT - T\Delta S^o_g(H^+) = (6.197 - 32.437)$ kJ mol^{-1} = −26.3 kJ mol^{-1} at 298.15 K and 1 atm.[73] The standard Gibbs free energy of solvation of HA and A^- in water [ΔG^o_{solv}(HA) and $\Delta G^o_{solv}(A^-)$] at their standard states (1 M ideal solution at 298 K) was calculated using the continuum solvation approach by Tomasi and his group, i.e., the PCM model, as implemented in the *Gaussian03* program.[41] For the standard Gibbs free energy of solvation of a proton in water, $\Delta G^o_{solv}(H^+)$, the experimental value of (−1103.4 ± 0.3 kJ mol^{-1})[74] was chosen.

In Scheme 4, where the solution phase Gibbs free energies for HA and A^- are calculated, while that of the proton is taken from an experimental measurements, the corrections for HA and A^- would cancel each other and thus would not alter any final results, neither the final pK_a values nor the final parameters of the solvation Gibbs free energy of proton, $\Delta G^o_{solv}(H^+)$.

The results for calculation of acidities in the gas phase and in aqueous solution at the MP2/6−311++G(d,p) level of theory for HU and NMHU are summarized in Table 6. With respect to the possible existence of several stable rotational conformers of HU and its structural analogues, the Gibbs free energy of deprotonation may be calculated between two arbitrary species. Those between two species with most similar structures might be of theoretical interest, but only the differences between the most stable species can have physical meaning and can be compared to experiments. Accordingly, only the most stable neutral and anionic forms of HU and NMHU were considered in the pK_a calculation.

M. Remko et al.[28] computed *N*-hydroxyurea to behave as *N*-acid in the gas phase at the CBS-QB3 level of theory. The results from this study show that HU is indeed a weak acid in the gas phase. In the absence of the gas-phase acidities of the HU and NMHU, the experimentally measured gas phase acidity of structurally related hydroxamic acid could be an interesting comparison of calculated Gibbs free energies of deprotonation with experimental data. The above-mentioned values computed in this study at the MP2/6−311++G(d,p) are consistent with the Gibbs free energy of Ventura et al.[65] for formohydroxamic acid (1311.3 kJ mol^{-1}). The substitution of the hydrogen atom in formohydroxamic acid by an amino group (electron donating substituent) leads to a considerable decrease of acidity relative to the parent acid. A similar decrease of acidity upon the amine substitution has been observed for carbonic acid,[75] thiocarboxylic acid[76] and silanoic acid.[77]

The results shown in Table 6 reveal that switching from the gas-phase to the PCM calculations strongly decreases the calculated pK_a values, and that the deprotonation processes also depend on the specific interactions of particular species with the solvent molecules through the hydrogen bonding. Analysis of calculated dipole moments of the isolated species HU and its water clusters (Table S5 of the Supporting Information) shows that the more hydrated HU species is, the smaller is dipole moment. Within the continuum model, stabilization energy is directly related to the magnitude of the dipole moment of a molecule. The dipole moments of the molecular structures affect the solvent by polarizing it, while the dielectric field created by the solvent and represented by its dielectric constant, and stabilizes the molecule. Thus, an important objective of this observation is to compare the solvation Gibbs free energies of isolated and hydrated species of HU calculated with the PCM method. For example, the *Z*-amide solvation energy varies from −26.2 kJ mol^{-1} when isolated, to −2.5 kJ mol^{-1} in the trihydrate. Similarly, the solvation energy of the *Z*-U$^-$O anion varies from −291.9 kJ mol^{-1} when isolated, to −185.3 kJ mol^{-1} in the trihydrate.

The results of aqueous phase calculations of the most probable deprotonation processes of *N*-hydroxyurea and its derivatives are compared (Table 6) with experimental data from Table 1. Unfortunately, even the smallest calculated pK_a values still greatly exceeds the experimentally determined ones, but there is a trend of approaching the experimental values by adding one and three water molecules in the first hydration shell of isolated species of neutral and anionic forms of HU and NMHU. This is even more so in going from isolated species to decahydrated species at the MP2/6−311G(d,p) level of theory (Table S10 of the Supporting Information). In both acids studied here, specific inclusion of additional water molecules lowers the computed pK_a values.

The difference between the theoretical and experimental values may be partly due to the already mentioned different methods for the evaluation of experimental and theoretical Gibbs free energies of ionization. Another reason for the observed discrepancy could be due to the fact that the actual structures of the acids in solution differ from those obtained from application of the continuum solvation model.[78] The computed pK_a values for the hydrated structures depend on the way of hydration of the ionisable group. Nevertheless, good agreement

between the experimental and calculated values for deprotonation processes in the gas-phase indicates that it is the solvation method that is responsible for the discrepancy between the experimental and QM results in aqueous solution.

Analysis of Deviations from the Linearity in ΔH_a vs ΔS_a. Once the most stable species involved in the deprotonation processes are defined (Tables 3, 4, and 5), we can turn our attention to the deviations from the linearity observed for the hydroxyureas. It is obvious from the disagreement between the experimental and theoretical pK_a values (Table 6) that the calculation of Gibbs free energies for deprotonation processes suffers from serious problems even upon inclusion of both the polarized continuum and the discrete water molecules. These problems could be caused by various factors including a lack of accounting for the second hydration sphere of investigated species wherein water molecules could have rather notable impact on the calculated values of Gibbs free energy of anionic species in water. From the observed agreement between the gas-phase experimentally determined pK_a values and the calculated ones, one may assume that calculation of the reaction enthalpies could be less sensitive and in turn less erroneous than the calculations of the entropies. Therefore, analysis of the relative reaction enthalpies could exemplify a simpler and more fruitful approach of finding the rationale behind the deviations from linearity of ΔH_a vs ΔS_a observed for HU and NMHU. However, attribution of the observed deviations to the differences in the reaction enthalpies has a meaning of addressing the problem mainly by invoking the different deprotonation sites of hydroxyureas, *i.e.*, the O- and N-deprotonation sites. Since in each of the deprotonation reactions a single proton is released, for satisfactory comparison of reaction enthalpies of the entire deprotonation processes, consideration of its thermodynamics is not necessary. Therefore, hereafter the term "apparent" is used to stress that the energetics of released proton is disregarded.

There are two molecular and three anionic species that can participate in the overall deprotonation of HU in water at 298.15 K: *E*-HU, *E*-HU·w, *Z*-U$^-$N1·w, *E*-U$^-$O·w, and, *E*-U$^-$O·3w. Among the molecular forms, *E*-HU, *E*-HU·w participate with 30% and 70%, while among the anions, *Z*-U$^-$N1·w, *E*-U$^-$O·w, and *E*-U$^-$O·3w participate with 94%, 4.4%, and 1.6%, respectively. Accordingly, there are six deprotonation paths that notably contribute to the overall deprotonation process: (i) *E*-HU + w → *Z*-U$^-$N1·w; $\Delta_r H_{app.}(i) = \Delta_f H(Z\text{-U}^-\text{N1}\cdot\text{w}) - \Delta_f H(E\text{-HU}) - \Delta_f H(\text{w}) = 1390$ kJ/mol, (ii) *E*-HU + w → *E*-U$^-$O·w; $\Delta_r H_{app.}(ii) = \Delta_f H(E\text{-U}^-\text{O}\cdot\text{w}) - \Delta_f H(E\text{-HU}) - \Delta_f H(\text{w}) = 1403$ kJ/mol, (iii) *E*-HU + 3w → *E*-U$^-$O·3w; $\Delta_r H_{app.}(iii) = \Delta_f H(E\text{-U}^-\text{O}\cdot 3\text{w}) - \Delta_f H(E\text{-HU}) - 3\Delta_f H(\text{w}) = 1153$ kJ/mol, (iv) *E*-HU·w → *Z*-U$^-$N1·w; $\Delta_r H_{app.}(iv) = \Delta_f H(Z\text{-U}^-\text{N1}\cdot\text{w}) - \Delta_f H(E\text{-HU}\cdot\text{w}) = 1427$ kJ/mol, (v) *E*-HU·w → *E*-U$^-$O·w; $\Delta_r H_{app.}(v) = \Delta_f H(E\text{-U}^-\text{O}\cdot\text{w}) - \Delta_f H(E\text{-HU}\cdot\text{w}) = 1441$ kJ/mol, and (vi) *E*-HU·w + 2w → *E*-U$^-$O·3w; $\Delta_r H_{app.}(vi) = \Delta_f H(E\text{-U}^-\text{O}\cdot 3\text{w}) - \Delta_f H(E\text{-HU}) - 2\Delta_f H(\text{w}) = 1536$ kJ/mol.

Assuming that the reaction enthalpy of deprotonation at the O-site causes no deviation from the theoretical line, i.e., the deviation is solely caused by the enthalpy of deprotonation at the N-site(s), we can calculate deviation from the apparent reaction enthalpy of each particular deprotonation path by taking the above calculated path participations as weighting factors:

$$\text{Est. dev. of}\Delta H_a = q_{Z\text{-U-N1}\cdot\text{w}}\{g_{E\text{-HU}}[K_1\Delta_r H_{app.}(ii) + K_2\Delta_r H_{app.}(iii) - \Delta_r H_{app.}(i)] + g_{E\text{-HU}\cdot\text{w}}[K_1\Delta_r H_{app.}(v) + K_2\Delta_r H_{app.}(vi) - \Delta_r H_{app.}(iv)]\} \quad (5)$$

In eq 5, $q_{Z\text{-U-N1}\cdot\text{w}}$ is participation of the N-deprotonation site ($q_{Z\text{-U-N1}\cdot\text{w}} + q_{(E\text{-U-O}\cdot\text{w} + E\text{-U-O}\cdot 3\text{w})} = 0.94 + 0.06 = 1$), $g_{E\text{-HU}}$ and $g_{E\text{-HU}\cdot\text{w}}$ are participations among the *E*-forms of HU ($g_{E\text{-HU}} + g_{E\text{-HU}\cdot\text{w}} = 0.3 + 0.7 = 1$), $K_1 = \gamma_{E\text{-U-O}\cdot\text{w}}/(\gamma_{E\text{-U-O}\cdot\text{w}} + \gamma_{E\text{-U-O}\cdot 3\text{w}})$, $K_2 = \gamma_{E\text{-U-O}\cdot 3\text{w}}/(\gamma_{E\text{-U-O}\cdot\text{w}} + \gamma_{E\text{-U-O}\cdot 3\text{w}})$, whereas $\gamma_{E\text{-U-O}\cdot\text{w}}$ (= 0.044) and $\gamma_{E\text{-U-O}\cdot 3\text{w}}$ (= 0.016) are participations of O-deprotonated monohydrate and trihydrate water clusters. Substitution of the above values into eq 5 predicts the deviation from the straight line of 10.7 kJ mol^{-1}. This value compares quite favorably to the experimentally observed deviation of 7.6 kJ mol^{-1}. A small "redundant" part of the deviation (3.1 kJ mol^{-1}) could be regarded negligible, but can also be attributed to the corresponding deviation in the reaction entropy due to the N-deprotonation site, of ~−10 J K^{-1} mol^{-1}.

The latter value can be checked easily by use of the data reported in Tables 3, 4, and S2 of the Supporting Information, and by taking into account the relative participations. The reaction entropies for each of the six deprotonation paths of hydroxyurea can be calculated as follows: $\Delta_r S_{app.}(i) = -7.96$ J K^{-1} mol^{-1}, $\Delta_r S_{app.}(ii) = -0.37$ J K^{-1} mol^{-1}, $\Delta_r S_{app.}(iii) = -0.22$ J K^{-1} mol^{-1}, $\Delta_r S_{app.}(iv) = +0.85$ J K^{-1} mol^{-1}, $\Delta_r S_{app.}(v) = +0.05$ J K^{-1} mol^{-1}, and $\Delta_r S_{app.}(vi) = -35.54$ J K^{-1} mol^{-1}. Assuming that the reaction entropies of the deprotonation at O-site cause no deviation, substitution in eq 6 yields estimation of the deviation in the deprotonation entropy at the N-site of +0.4 J K^{-1} mol^{-1}. The obtained value indicates that in fact both deprotonation sites can equally contribute to the deviation from linearity eventually caused by the entropy of deprotonation.

$$\text{Est. dev. of}\Delta S_a = q\{g_{E\text{-HU}}[K_1\Delta_r S_{app.}(ii) + K_2\Delta_r S_{app.}(iii) - \Delta_r S_{app.}(i)] + g_{E\text{-HU}\cdot\text{w}}[K_1\Delta_r S_{app.}(v) + K_2\Delta_r S_{app.}(vi) - \Delta_r S_{app.}(iv)]\} \quad (6)$$

Taking into account simplicity of the above approach that ignores numerous subtle effects which could affect the deprotonation process (for instance: structure of the second hydration sphere, possible errors in the local dielectric constant of polarizable medium, energetics of ion pairing, etc.), one can conclude that the participation of the N- and O-sites in deprotonation of HU offers a reasonable explanation for deviation from the reported linear relationship between ΔH_a and ΔS_a.

In the case of NMHU, our calculations show that only O-site contributes to the deprotonation in water (Table 5), making worthless the above analysis of the observed deviation based on the enthalpy change associated with the change of deprotonation sites. The observed deviation must be mainly caused by unexpectedly negative reaction entropy of the NMHU deprotonation at the O-site. Assuming no deviation in the reaction enthalpy, a rough estimation shown in Table 2 predicts the deviation from the ΔH_a vs ΔS_a plot by −21 J mol^{-1} K^{-1}. Although the entropy values for the deprotonation processes are calculated with a high uncertainty, the above-mentioned disregard of the proton thermodynamics can make at least comparison of the apparent reaction entropies more reliable. Relating only the entropies of molecular and anionic forms of hydroxyureas may cancel out many of the error-introducing factors.

There are two molecular and two anionic species that can participate in the overall deprotonation of NMHU in water at 298.15 K: *E*-NMHU, *E*-NMHU·w, *E*-NMU$^-$O·w, and *E*-NMU$^-$O·3w. Among the molecular forms, *E*-NMHU and *E*-NMHU·w participate with 32% and 68%, while among the anions, *E*-NMU$^-$O·w, and *E*-NMU$^-$O·3w participate with 37% and 63%, respectively. Accordingly, there are four deprotonation paths that notably contribute to the overall deprotonation

process: (i) *E*-NMHU + w → *E*-NMU$^-$O·w; $\Delta_r S_{app.}$(i) = S(*E*-NMU$^-$O·w) − S(*E*-NMHU) − S(w) = −3.83 J K^{-1} mol^{-1}, (ii) *E*-NMHU + 3w → *E*-NMU$^-$O·3w; $\Delta_r S_{app.}$(ii) = S(*E*-NMU$^-$O·3w) − S(*E*-NMHU) − S(3w) = −7.59 J K^{-1} mol^{-1}, (iii) *E*-NMHU·w → *E*-NMU$^-$O·w; $\Delta_r S_{app.}$(iii) = S(*E*-NMU$^-$O·w) − S(*E*-NMHU) = −0.61 J K^{-1} mol^{-1}, (iv) *E*-NMHU·w + 2w → *E*-NMU$^-$O·3w; $\Delta_r S_{app.}$(iv) = S(*E*-NMU$^-$O·3w) − S(*E*-NMHU·w) − S(3w) = −18.26 J K^{-1} mol^{-1}. Taking into account participations of the species, calculations at the MP2/6−311++G(d,p) level of theory yield the apparent deprotonation entropy of −30 J K^{-1} mol^{-1}. However, eventual proportion of the deviation can be estimated only by comparing this value to the analogously calculated apparent entropy change for the deprotonation reaction of hydroxyurea, for the comparison eliminates the thermodynamics of proton. Taking the above values for entropy of each participating species of hydroxyurea, we calculate the apparent entropy of deprotonation as −43 J K^{-1} mol^{-1}. Since the deviation from the linearity can be covered by −10 J K^{-1} mol^{-1}, −33 J K^{-1} mol^{-1} apparent entropy change corresponds to no deviation from linearity for HU. Unfortunately, the meaning of such an analysis is that for NMHU the analogously calculated apparent entropy change of −30 J K^{-1} mol^{-1} should cause no deviation at all.

Experimental Section

Materials. Betainohydroxamic acid[39] and *N*-methylhydroxyurea[80] were synthesized by previously published procedures and the structure was confirmed by means of FT-IR and NMR spectroscopy. Acetohydroxamic acid (Aldrich), benzohydroxamic acid, (Merck) and hydroxyurea (Sigma) and all other reagents were of analytical grade and were used without further purification. All solutions were prepared using water twice distilled from alkaline $KMnO_4$ in an all-glass apparatus.

Instrumentation. Titrations were performed using Mettler Toledo DL55 automatic titrator equipped with Mettler DG-111SC combined glass pH electrode and Mettler DV910 10 mL glass burette with 0.3% accuracy. Temperature was kept constant using a Haake DC10-K10 water bath with 0.02 °C accuracy.

Methods. Stock solutions of hydroxamic acids (0.005 M in 2 M $NaClO_4$) were prepared by weighing appropriate amounts of hydroxamic acid and $NaClO_4$, diluted in CO_2-free water and filled to volume. A 25.00 ± 0.03-mL portion of the stock solution was placed in a water-jacketed cell connected to the thermostat and titrated against 0.2 M standard CO_2-free NaOH solution in an argon saturated atmosphere. All solutions were mixed for 15 min for temperature equalization before titration. Addition of NaOH was made in 0.05 mL increments and the resulting electrode potential values recorded. The glass electrode was standardized with buffers of known pH at each temperature. Obtained pH values were used in evaluation of K_a values by SUPERQUAD.[81]

Computational Details. The *Gaussian03* program package has been employed in all the calculations. Initial geometries of the water clusters of the HU and NMHU were built using GaussView 3.09, guided by the results of the clusters with fewer water molecules. Water molecules were placed in a variety of locations to sample the various arrays of hydrogen-bonding networks available between hydroxamate moiety and water and between water molecules. The molecular geometries of all neutral and anionic isolated species of *N*-hydroxyurea and *N*-methylhydroxyurea, as well as their associates with one, three, and ten water molecules were fully optimized with respect to the energy without any conformational or symmetry constraints at the quantum mechanical ab initio levels. Correlation energy was included using full (i.e., all electrons) second-order Møller−Plesset perturbation theory (MP2). Ab initio calculations were performed at the MP2 level of theory employing the 6−311++G(d,p) basis set. The nature of the stationary points was verified by computations of the harmonic frequencies at the same levels of theory. The computed harmonic frequencies were used to evaluate zero-point energies (ZPEs), thermal corrections to Gibbs free energies, as well as the enthalpy and entropy contributions at 298.15 K. In the case of compounds existing in several conformations, all possibilities were examined. Solvent effects in water have been calculated by means of the Tomasi's polarized continuum model (PCM) in which the solvent is considered as a continuum dielectric, characterized by a constant permittivity. The PCM method was directly applied to the neutral and anionic forms of hydroxamic acids, as implemented in the *Gaussian03* package, using the same levels of theory. The cavity radii are those recommended for the UAHF model. The solvent dielectric constant has been set at 78.5 for T = 298.15 K. Owing to high computational costs, the calculations on clusters with ten water molecules presented in this work were carried out employing 6−311G(d,p) basis set with no added diffuse functions at the MP2 level of theory. Manual searches for the most stable clusters investigated at the both theory levels were restricted to no more than three water molecules. In applying the Saunders's stochastic method, a starting structure is subjected to a "kick", which moves each atom in a random direction over a random distance within a sphere of given radius (R), which represent the maximal kick size. Optimization of the kicked structure with a quantum mechanical optimizer could take it back to the initial structure, or it can be refined to give a different isomer. We searched for all possible minima of neutral and anionic complexes of HU and NMHU with 10 water molecules employing the Saunders's stochastic method with kicks ranging from 0.7 to 1.1 Å. However, some selected coordinates (those of neutral or anionic form of hydroxyurea and NMHU) were frozen during the kick procedure. The method generates up to 500 unbiased starting geometries that were submitted for optimization with Gaussian03 at the BP86/I level of theory. While many jobs die quickly (the atoms are too close, or the self-consistent field convergence is not achieved) and the other jobs do not achieve geometrical convergence, the completed optimizations yielded in ∼30%. The energies of these minima ranged over 500 kJ mol^{-1}. The most stable structures, which were in energy span of 20 kJ mol^{-1}, were reoptimized at the MP2/6−311G(d,p) level of theory. For the basis set superposition error (BSSE), the complexes with one and three water molecules were completely optimized without any geometric restraints, and we used the two (CP2) and four (CP4) fragment definitions of CP for the hydration of AH and A$^-$. For CP4, we divide the complexes into four fragments, one of which is neutral or anionic form of hydroxyureas, whereas the other three are water molecules.

Conclusions

On the basis of the excellent linearity of the ΔH_a vs. ΔS_a plot, obtained by a thorough investigation of temperature dependence of pK_a for series of *C*- and *N*-substituted hydroxamic acids, Crumbliss and co-workers proposed the deprotonation for all of hydroxamic acids studied to occur by loss of −O*H* proton. Hence, the deviations observed for HU and NMHU raise a question of the dissociation site of hydroxureas in water, pointing to the $-NH_2$ site that is also a common functionality for both hydroxyureas. Although NMHU has two and HU even

three deprotonation sites, our potentiometric measurements confirm previous findings that HU[79] and NMHU behave as weak acids with a single $pK_a \approx 10$. We obtain a difference between pK_a of HU and NMHU, $pK_a(HU) - pK_a(NMHU) = 0.36$, that is very close to the difference reported for the AcHA/NMAcHA couple, $pK_a(AcHA) - pK_a(NMAcHA) = 0.39$.[22] Thus, the differences in experimental Gibbs free energies for dissociation of HU/NMHU, $\Delta(\Delta_r G)_{HU/NMHU} = 2.5$ kJ mol^{-1}, and AcHA/NMAcHA, $\Delta(\Delta_r G)_{AcHA/NMAcHA} = 2.2$ kJ mol^{-1}, match each other within the experimental uncertainties. At first glance, this may appear in accord with the suggestion that the hydration of $R_1-C=O$ ($H_2N-C=O$ in hydroxyureas) moiety has no, or only minor, effect on the pK_a values, because the deprotonation of hydroxamic acids in aqueous solution occurs at the $-OH$ site. However, in contrast to the similarity of $\Delta(\Delta_r G)$ values for the deprotonation of HU/NMHU and AcHA/NMAcHA, the reaction entropies reveal quite different behavior of these two pairs of hydroxamic acids. A small difference between the reaction entropies for ionization of HU and NMHU ($\Delta(\Delta_r S) = 2$ J K^{-1} mol^{-1}) compared to the much larger difference for ionization of AcHA and NMAcHA ($\Delta(\Delta_r S) = 40$ J K^{-1} mol^{-1}) point to a possible influence of electronic properties of $-NH_2$ as the $-R_1$ group on the hydration of $R_1-C=O$ moiety and in turn on the deprotonation of hydroxyureas.

Previous NMR and theoretical studies indicate that in aqueous solutions HU is predominantly the $-O\boldsymbol{H}$ deprotonated, while the gas phase ab initio calculations show that $U-N1^-$ anion is the most stable due to a strong $O-H\cdots\cdots N^-$ intramolecular hydrogen bonding.[26,28,62] Our calculations for HU confirm contribution of two deprotonation sites in the aqueous medium. The conformations of flexible molecules and their relative stabilities can be very sensitive to the type of electron correlation used, because of the importance of dispersion contributions and to the basis set employed, as large basis sets are required to avoid intramolecular BSSE. The more reliable calculations reported in this paper required considerable computational resources necessary to balance BSSE and dispersion errors that are likely to be problematic. Since our potentiometric results demonstrate that HU and NMHU exhibit very similar acidities, and taking into account that presence of $-CH_3$ group in NMHU molecule leaves only $-NH_2$ as the N-deprotonation site, one might ruled out the N—H hydroxamate moiety as a possible deprotonation site and concluded that $-NH_2$ acts as the N-deprotonation site in both compounds causing their similar acidities. Yet on contrary to that assumption, our calculations reveal that the most favorable deprotonation site in HU is the nitrogen of hydroxylamine group ($-N\boldsymbol{H}-OH$), whereas in NMHU, the most acidic site in aqueous solution is the oxygen of hydroxylamino group ($-NH-O\boldsymbol{H}$).

Therefore, along with experimental observation of only one pK_a for both hydroxyureas, the theoretical predictions of two deprotonation sites in HU can serve as a plausible explanation for the observed deviations from linearity in the $\Delta_r H_a$ vs $\Delta_r S_a$ plot. A single O-deprotonation site predicted for NMHU makes search for a plausible explanation of the deviation from linearity more complex and the use of the above-proposed calculation model inadequate. Therefore, the explanation for NMHU will have to wait some additional experimental evidence, which may bring some more light into depiction of the acid−base behavior of that compound.

Acknowledgment. The authors appreciate financial support from Ministry of Science, Education, and Sport of the Republic of Croatia through Grant, No. 006-0061247-0009. We are also grateful to Dr. Michael Bühl for fruitful discussions.

Supporting Information Available: Tables: Calculated enthalpies and Gibbs free energies in the gas phase and in water (using the PCM method) of studied neutral species of HU and NMHU obtained at the MP2/6−311G(d,p) and MP2/6−311++G(d,p) levels of theory; NPA charges calculated for molecular and anionic species of HU and NMHU at the MP2/6−311++G(d,p) level of theory: Wiberg bond indices calculated for molecular and anionic species of HU and NMHU at the MP2/6−311++G(d,p) level of theory; Dipole moments (in Debye) calculated for molecular and anionic species of HU and NMHU at the MP2/6−311G(d,p) and MP2/6−311++G(d,p) levels of theory; Calculated reaction Gibbs free energies for selected deprotonation processes of HU in the gas phase and in aqueous solution with corresponding pK_a values at 298.15 K at the MP2/6−311G(d,p) level of theory; Cartesian Coordinates in Å (optimized at the MP2/6−311G(d,p), optimized at the MP2/6−311++G(d,p), optimized at the PCM/MP2/6−311++G(d,p), CP-optimized at the MP2/6−311++G(d,p) level), xyz format. Figures: The most stable neutral and anionic complexes of HU with ten water molecules optimized at the MP2/6−311G(d,p) level of theory; Starting and resulting zwitterionic structure of NMHU for optimization procedure in the gas-phase at the MP2/6−311++G(d,p) level of theory. This material is available free of charge via the Internet at http://pubs.acs.org.

References and Notes

(1) Kaczka, E. A.; Gitterman, C. O.; Dulaney, E. L.; Folkers, K. *Biochemistry* **1962**, *1*, 340–343.

(2) Matzanke, B. F.; Mueller-Matzanke, G.; Raymond, K. N. *Iron Carriers and Iron Proteins*; VCH Publishers: New York, 1989, Vol. 5, pp 1−121.

(3) Hersko, C.; Gordeuk, V. R.; Thuma, P. E.; Thenacho, E. N.; Spira, D. T.; Hider, R. C.; Peto, T. E. A.; Drittenham, G. M. *J. Inorg. Biochem.* **1992**, *47*, 267–277.

(4) Rogers, H. J. *Iron Transport in Microbes, Plants and Animals*; VCH Publishers: New York, 1987, pp 223−233.

(5) Ghio, A. J.; Kennedy, T. P.; Whorton, R. A.; Crumbliss, A. L.; Hatch, G. E.; Hoidal, J. R. *Am. J. Physiol.* **1992**, *263*, 511–518.

(6) Crumbliss, A. L. *Handbook of Microbial Iron Chelates*, CRC Press: Boca Raton, 1991, pp 177−233.

(7) Leoni, F.; Zaliani, A.; Bertolini, G.; Porro, G.; Pagani, P.; Pozzi, P.; Dona, G.; Fossati, G.; Sozzani, S.; Azam, T.; Bufler, R.; Fantuzzi, G.; Goncharav, I.; Kim, S. H.; Pomerantz, B. J.; Reznikov, L. L.; Siegmund, B.; Dinarello, C. A.; Mascagni, P. *Proc. Natl. Acad. Sci.* **2002**, *99*, 2995–3000.

(8) Clare, B. W.; Scozzafava, A.; Supuran, C. T. *J. Med. Chem.* **2001**, *44*, 2253–2258.

(9) Onishi, H. R.; Pelak, B. A.; Gerckens, L. S.; Silver, L. L.; Kahan, F. M.; Chen, M. H.; Patchett, A. A.; Galloway, S. M.; Hyland, S. A.; Anderson, M. S.; Raetz, C. R. H. *Science* **1996**, *274*, 980–982.

(10) Clements, J. M.; Beckett, R. P.; Brown, A.; Catlin, G.; Labell, M.; Palan, S.; Thomas, W.; Whittaker, M.; Wood, S.; Salama, S.; Baker, P. J.; Rodgers, H. F.; Barynin, V.; Rice, D. W.; Hunter, M. G. *Antimicrob. Agents Chemother.* **2001**, *45*, 563–570.

(11) Kikuchi, T.; Itoh, F.; Toyota, M.; Suzuki, H.; Yamamoto, H.; Fujita, M.; Hosokawa, M.; Imai, K. *Int. J. Cancer* **2002**, *97*, 272–277.

(12) Komatsu, Y.; Tomizaki, K. Y.; Tsukamoto, M.; Kato, T.; Nishino, N.; Sato, S.; Yamori, T.; Tsuruo, T.; Furumai, R.; Yoshida, M.; Horinouchi, S.; Hayashi, H. *Cancer Res.* **2001**, *61*, 4459–4466.

(13) Nyholm, S.; Thelander, L.; Graeslund, A. *Biochemistry* **1993**, *32*, 11569–11574.

(14) Zhou, B.; Mi, S.; Mo, X.; Shih, J.; Tsai, J.; Hu, E.; Hsu, M.; Kay, K.; Yen, Y. *Anticancer Res.* **2002**, *22*, 1369–1377.

(15) Huang, P.-H.; You, J.-Y.; Hsu, H.-C. *Haematologica* **2002**, *32*, 87–91.

(16) Mason, W. P.; Gentili, F.; Macdonald, D. R.; Hariharan, S.; Cruz, C. R.; Abrey, L. E. *J. Neurosurg.* **2002**, *97*, 341–347.

(17) Charache, S.; Terrin, M. L.; Moore, R. D.; Dover, G. J.; Barton, F. B.; Eckert, S. V.; McMahon, R. P.; Bonds, D. R. *New Engl. J. Med.* **1995**, *332*, 1317–1322.

(18) Ferguson, R. P.; Arun, A.; Carter, C.; Walker, S. D.; Castro, O. *Am. J. Hematol.* **2002**, *70*, 326–330.

(19) Senent, M. L.; Niño, A.; Munoz Caro, C.; Ibeas, S.; Garcia, B.; Leal, J. M.; Secco, F.; Ventirini, M. *J. Org. Chem.* **2003**, *68*, 6535–6542.

(20) Kakkar, R.; Grover, R.; Chadha, P. *Org. Biomol. Chem.* **2003**, *1*, 2200–2206.
(21) Bagno, A.; Comuzzi, C.; Scorrano, G. *J. Am. Chem. Soc.* **1994**, *116*, 916–924.
(22) Monzyk, B.; Crumbliss, A. L. *J.Org. Chem.* **1980**, *45*, 4670–4675.
(23) Larsen, I. K. *Acta Crystallogr., Sect. B* **1988**, *44*, 527–533.
(24) Brown, D. A.; Coogan, R. A.; Fitzpatrick, N. J.; Glass, W. K.; Abuksima, D. E.; Shields, L.; Ahlgrén, M.; Smolander, K.; Pakkanen, T. T.; Pakkanen, T. A.; Peräkkylä, M. *J. Chem. Soc., Perkin Trans.* **1996**, *2*, 2673–2679.
(25) La Manna, G.; Barone, L. *Int. J. Quantum Chem.* **1996**, *57*, 971–974.
(26) Bagno, A.; Comuzzi, C. *Eur. J. Org. Chem.* **1999**, *1*, 287–295.
(27) Remko, M.; Lyne, P. D.; Richards, W. G. *Phys. Chem. Chem. Phys.* **2000**, *2*, 2511–2514.
(28) Remko, M.; von Lieth, C.-W. *Struct. Chem.* **2004**, *15*, 285–294.
(29) Di Gregorio, G.; La Mamna, G.; Paniagua, J. C.; Vilaseca, E. *J. Mol. Struct. (THEOCHEM)* **2000**, *673*, 87–92.
(30) Remko, M.; Lyne, P. D.; Richards, W. G. *Phys. Chem. Chem. Phys.* **1999**, *1*, 5353–5357.
(31) Senthilkumar, L.; Kolandaivel, P. *J. Mol. Struct.* **2006**, *791*, 149–157.
(32) Ramondo, F.; Bencivenni, L.; Rossi, V.; Caminiti, R. *J. Mol. Struct. (THEOCHEM)* **1992**, *271*, 185–211.
(33) Jabalameli, A.; Zhanpeisov, N. U.; Nowek, A.; Sullivan, R. H.; Leszczynski, J. *J. Phys. Chem. A* **1997**, *101*, 3619–3625.
(34) Mora-Diez, N.; Senent, M. L.; García, B. *Chem. Phys.* **2006**, *324*, 350–358.
(35) Berkenkopf, J. W.; Weichman, B. M. *Eur. J. Pharmacol.* **1991**, *193*, 29–34.
(36) Navarra, P.; Preziosi, P. *Crit. Rev. Oncol./Hematol.* **1998**, *29*, 248–255.
(37) Kayyalii, R.; Pannala, A. S.; Khodr, H.; Hider, R. C. *Biochem. Pharamcol.* **1998**, *55*, 1327–1332.
(38) Gale, G. R. *Biochem. Pharmacol.* **1968**, *17*, 235–240.
(39) Biruš, M.; Kujundžič, N.; Pribanič, M.; Tabor, Z. *Croat. Chem. Acta* **1984**, *57*, 313–324.
(40) Vinkovič Vrček, I.; Biruš, M.; Buehl, M. *Inorg. Chem.* **2007**, *46*, 1488–1501.
(41) Frisch, M. J.; Trucks, G. W.; Schlegel, H. B.; Scuseria, G. E.; Robb, M. A. Cheeseman, J. R.; Montgomery, J. A., Jr.; Vreven, T.; Kudin, K. N.; Burant, J. C.; Millam, J. M.; Iyengar, S. S.; Tomasi, J.; Barone, V.; Mennucci, B.; Cossi, M.; Scalmani, G.; Rega, N.; Petersson, G. A.; Nakatsuji, H.; Hada, M.; Ehara, M.; Toyota, K.; Fukuda, R.; Hasegawa, J.; Ishida, M.; Nakajima, T.; Honda, Y.; Kitao, O.; Nakai, H.; Klene, M.; Li, X.; Knox, J. E.; Hratchian, H. P.; Cross, J. B.; Bakken, V.; Adamo, C.; Jaramillo, J.; Gomperts, R.; Stratmann, R. E.; Yazyev, O.; Austin, A. J.; Cammi, R.; Pomelli, C.; Ochterski, J. W.; Ayala, P. Y.; Morokuma, K.; Voth, G. A.; Salvafdor, P.; Dannenberg, J. J.; Zakrzewski, V. G.; Dapprich, S.; Daniels, A. D.; Strain, M. C.; Farkas, O.; Malick, D. K.; Rabuck, A. D.; Raghavachari, K.; Foresman, J. B.; Ortiz, J. V.; Cui, Q.; Baboul, A. G.; Clifford, S.; Cioslowski, J.; Stefanov, B. B.; Liu, G.; Liashenko, A.; Piskorz, P.; Komaromi, I.; Martin, R. L.; Fox, D. J.; Keith, T.; Al-Laham, M. A.; Peng, C. Y.; Nanayakkara, A.; Challacombe, M.; Gill, P. M. W.; Johnson, B.; Chen, W.; Wong, M. W.; Gonzalez, C.; Pople, J. A. *Gaussian 03*; Gaussian, Inc.: Wallingford, CT, 2004.
(42) (a) Tomasi, J.; Persico, M. *Chem. Rev.* **1994**, *94*, 2027–2094. (b) Barone, M.; Cossi, B.; Mennucci, B.; Tomasi, J. *J. Chem. Phys.* **1997**, *107*, 3210–3221.
(43) Cramer, C. J.; Truhlar, D. G. *Chem. Rev.* **1999**, *99*, 2161–2200.
(44) Bera, P. P.; Sattelmeyer, K. W.; Saunders, M.; Schaefer III, H. F.; Schleyer, P. v. R. *J. Phys. Chem. Lett. A* **2006**, *110*, 4287–4290.
(45) Saunders, M. *J. Comput. Chem.* **2004**, *25*, 621.
(46) Saunders, M. *J. Am. Chem. Soc.* **1987**, *109*, 3150–3157.
(47) van Duijneveldt, F. B. Basis set superposition error. In *Molecular Interactions*; Scheiner, S., Ed.; Wiley: Chichester, UK, 1997; pp 81−104.
(48) Boys, S. F.; Bernardi, F. *Mol. Phys.* **1970**, *19*, 553–559.
(49) Simon, S.; Duran, M.; Dannenberg, J. J. *J. Chem. Phys.* **1996**, *105*, 11024–11031.
(50) Glendening, E. D.; Reed, A. E.; Carpenter, J. E.; Weinhold, F. *NBO (version 3.1)*.
(51) Brink, C. P.; Crumbliss, A. L. *J. Org. Chem.* **1982**, *47*, 1171–1176.
(52) Brink, C. P.; Crumbliss, A. L. *Inorg. Chem.* **1984**, *23*, 4708–4718.
(53) Brink, C. P.; Fish, L. L.; Crumbliss, A. L. *J. Org. Chem.* **1985**, *50*, 2277–2281.
(54) Kapp, J.; Remko, M.; Schleyer, P. v. R. *Inorg. Chem.* **1997**, *36*, 4241–4246.
(55) Bracher, B. H.; Small, R. W. H. *Acta Crystallogr.* **1970**, *26*, 1705–1709.
(56) Remko, M. *J. Phys. Chem. A* **2002**, *106*, 5005–5010.
(57) Reed, A. E.; Curtiss, L. A.; Weinhold, F. *Chem. Rev.* **1988**, *88*, 899–926.
(58) Cotta Ramusino, M. *J. Mol. Struct. (THEOCHEM)* **1998**, *427*, 237–242.
(59) Salvador, P.; Duran, M.; Dannenberg, J. J. *J. Phys. Chem. A* **2002**, *106*, 6883–6889, and references therein.
(60) Kobko, N.; Dannenberg, J. J. *J. Phys. Chem. A* **2001**, *105*, 1944–1950.
(61) Bagno, A.; Scorrano, G. *Acc. Chem. Res.* **2000**, *33*, 609–616.
(62) Decouzon, M.; Exner, O.; Gal, J. F.; Maria, P. C. *J. Org. Chem.* **1990**, *55*, 3980–3981.
(63) Brown, D. A.; Glass, W. K.; Mageswaran, R.; Girmany, B. *Magn. Reson. Chem.* **1988**, *26*, 970–973.
(64) García, B.; Ibeas, S.; Leal, J. M.; Secco, F.; Venturini, M.; Senent, M. L.; Niño, A.; Muñoz-Caro, C. *Inorg. Chem.* **2005**, *44*, 2908–2919.
(65) Ventura, O. N.; Rama, J. B.; Turi, L.; Dannenberg, J. J. *J. Am. Chem. Soc.* **1993**, *115*, 5754–5761.
(66) Yen, S. J.; Lin, C. Y.; Ho, J. *J. Phys. Chem. A* **2000**, *104*, 11771–11776.
(67) ISI Web of Knowledge, http://isiknowledge.com/.
(68) Liptak, M. D.; Shields, G. C. *Int. J. Quantum Chem.* **2001**, *85*, 727–741.
(69) Toth, A. M.; Liptak, M. D.; Phillips, D. L.; Shields, G. C. *J. Chem. Phys.* **2001**, *114*, 4595–4606.
(70) Liptak, M. D.; Shields, G. C. *J. Am. Chem. Soc.* **2001**, *123*, 7314–7319.
(71) Liptak, M. D.; Gross, K. C.; Seybold, P. G.; Shields, G. C. *J. Am. Chem. Soc.* **2002**, *124*, 6421–6427.
(72) Atkins, P. *Physical Chemistry*, 6th ed.; Oxford University Press, UK 1998.
(73) Topol, I. A.; Tawa, G. J.; Burt, S. K.; Rashin, A. A. *J. Phys. Chem. A* **1997**, *101*, 10075–10081.
(74) Tissandier, M. D.; Cowen, K. A.; Feng, W. Y.; Gundlach, E.; Cohen, M. H.; Earhart, A. D.; Coe, J. V.; Tuttle, T. R., Jr. *J. Phys. Chem. A* **1998**, *102*, 7787–7794.
(75) Remko, M. *J. Mol. Struct. (THEOCHEM)* **1999**, *492*, 203–208.
(76) Remko, M.; Liedl, K. R.; Rode, B. M. *J. Mol. Struct. (THEOCHEM)* **1997**, *418*, 179–187.
(77) Remko, M. *Mol. Phys.* **1999**, *96*, 1677–1679.
(78) Adam, K. R. *J. Phys. Chem. A* **2002**, *106*, 11963–11972.
(79) Kofod, H.; Huang, T.-Y. *Acta Chem. Scand.* **1954**, *8*, 494–502.
(80) Mathieson, O. UK Pat. GB930844(1963), C07C275/64 C07C275.
(81) Gans, P.; Sabatini, A.; Vacca, A. *J. Chem. Soc., Dalton Trans.* **1985**, 1195–1200.

JP804925B